Anal Bioanal Chem (2015) 407:961–972
DOI 10.1007/s00216-014-8247-0

RESEARCH PAPER

High-performance liquid chromatographic enantioseparation of cationic 1,2,3,4-tetrahydroisoquinoline analogs on *Cinchona* alkaloid-based zwitterionic chiral stationary phases

István Ilisz · Nóra Grecsó · Ferenc Fülöp · Wolfgang Lindner · Antal Péter

Received: 25 June 2014 / Revised: 22 September 2014 / Accepted: 7 October 2014 / Published online: 19 October 2014

Abstract The stereoisomers of 1,2,3,4-tetrahydroisoquinoline analogs were resolved for the first time by applying a polar ionic mobile phase on a quinine or a quinidine moiety fused with a chiral sulfonic acid-type chiral selector immobilized on silica [Chiralpak ZWIX(+)™ and Chiralpak ZWIX(−)™]. The effects of the nature and concentrations of the mobile phase components and additives and temperature on the retention and enantioseparation on the investigated chiral columns were studied. Experiments were performed in the temperature range 10–50 °C. Thermodynamic parameters were calculated from plots of ln α versus 1/*T*. The separations were generally enthalpy-controlled, but entropy-controlled separation was also observed below 30 °C. The enantiomer elution order was determined in some cases and was observed to be opposite on the ZWIX(+)™ and ZWIX(−)™ columns. Our results contribute to a better understanding of the enantiorecognition mechanism of chiral bases with chiral zwitterionic selectors.

Keywords High-performance liquid chromatography · Enantioseparation of 1,2,3,4-tetrahydroisoquinoline analogs · Zwitterionic selectors · Thermodynamics of enantioseparation

Published in the topical collection celebrating *ABCs 13th Anniversary.*

Electronic supplementary material The online version of this article (doi:10.1007/s00216-014-8247-0) contains supplementary material, which is available to authorized users.

I. Ilisz · N. Grecsó · A. Péter (✉)
Department of Inorganic and Analytical Chemistry, University of Szeged, Dóm tér 7, 6720 Szeged, Hungary
e-mail: apeter@chem.u-szeged.hu

N. Grecsó · F. Fülöp
Institute of Pharmaceutical Chemistry, University of Szeged, Eötvös u. 6, 6720 Szeged, Hungary

W. Lindner
Department of Analytical Chemistry, University of Vienna, Währingerstrasse 38, 1090 Vienna, Austria

Introduction

Compounds containing a 1,2,3,4-tetrahydroisoquinoline (Tiq) skeleton (Fig. 1) are important building blocks of naturally occurring alkaloids [1] and are of great importance in synthetic chemistry and drug research for their potential pharmaceutical activity [2]. Some commercially available drugs such as the antitussive noscapin and the antitumor agent trabectedin (as Yondelis®) contain enantiomerically pure Tiq as a key structural unit. Lee et al. [3] reported the anti-HIV effects of (1*R*)-coclaurine and (1*S*)-norcoclaurine, naturally occurring alkaloids isolated from *Nelumbo nucifera*. Trimetoquinol and its 3′,5′-diiodo derivative are β-adrenoceptor agonists and the (*S*)-trimetoquinol is in use as a bronchodilatory agent [4]. Tiq compounds, e.g., [(*R*)-salsolinol], have been detected in the human brain and intraventricular fluid, and their possible roles in the pathogenesis of Parkinson's disease have been discussed [5]. 1-Methyl- and 1-phenyl-Tiq are of importance in the prevention of Parkinson's and other neurological diseases [6]. Analyte **9** (Fig. 1) is an important intermediate in the preparation of the expectorant emetin [7], and **10** is a potential intermediate for the preparation of crispine A, which displays high biological activity against the human cancer cell lines SKOV3, KB, and HeLa [8].

As the behavior of Tiq derivatives in biological systems depends strongly on their stereochemistry, there is a clear need for precise separation and identification methods through which the enantiomeric excess can be analyzed and the absolute configurations can be assigned.

Chiral separations of Tiq analogs have been performed by both indirect and direct analytical methodologies. The gas chromatographic (GC) indirect separation of salsolinol enantiomers has been achieved through the application of *N*-methyl-*N*-trimethylsilyl trifluoracetamide [9] and (*R*)-(−)-2-phenylbutyryl chloride [10] as chiral derivatizing agents (CDAs), while high-performance liquid chromatography

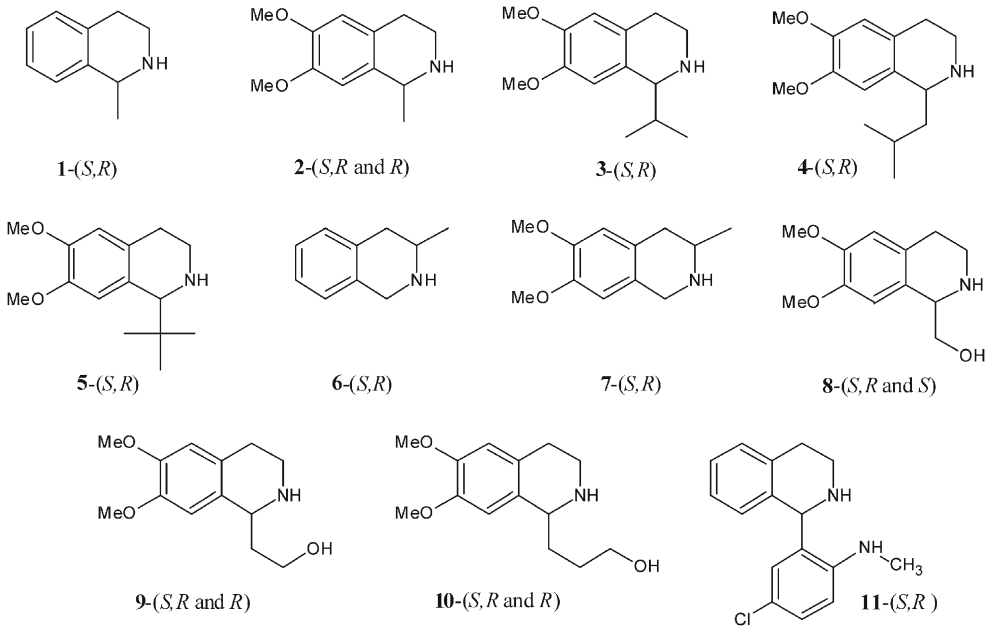

Fig. 1 Structures of analytes **1**, 1-methyl-1,2,3,4-tetrahydroisoquinoline; **2**, 6,7-dimethoxy-1-methyl-1,2,3,4-tetrahydroisoquinoline; **3**, 6,7-dimethoxy-1-(propan-2-yl)-1,2,3,4-tetrahydroisoquinoline; **4**, 6,7-dimethoxy-1-(2-methylpropyl)-1,2,3,4-tetrahydroisoquinoline; **5**, 1-*tert*-butyl-6,7-dimethoxy-1,2,3,4-tetrahydroisoquinoline; **6**, 3-methyl-1,2,3,4-tetrahydroisoquinoline; **7**, 6,7-dimethoxy-3-methyl-1,2,3,4-tetrahydroisoquinoline; **8**, (6,7-dimethoxy-1,2,3,4-tetrahydroisoquinolin-1-yl)methanol; **9**, 2-(6,7-dimethoxy-1,2,3,4-tetrahydroisoquinolin-1-yl)ethanol; **10**, 3-(6,7-dimethoxy-1,2,3,4-tetrahydroisoquinolin-1-yl)propan-1-ol; and **11**, 4-chloro-*N*-methyl-2-(1,2,3,4-tetrahydroisoquinolin-1-yl)aniline

(HPLC) has been carried out with isothiocyanate-based CDAs [11].

The direct separation in HPLC involved the application of β-cyclodextrins or sulfated β-cyclodextrins as chiral mobile phase additives (CMPAs) [12–14]. CMPAs have also been applied in capillary electrophoresis (CE) methods with hydroxypropyl-β-cylodextrin as chiral selector for the enantioseparation of (*R,S*)-salsolinol [15] or with β-cylodextrin for enantioseparation of dopamine-derived neurotoxins [16] or for the separation of the diastereomers of (*R,S*)-Tiq-3-carboxylic acid derivatized with (*R*)-4-nitro-7-(3-aminopyrrolidin-1-yl)-2,1,3-benzoxadiazole [17]. A CE method and a computational modeling study have been used to investigate the complex formation of Tiq analogs with β-cyclodextrin [18]. Salsolinol enantiomers were separated through the application of chiral stationary phases (CSPs) containing β-cyclodextrin-type chiral selectors in GC [19] and in HPLC [20–24]. The normal-phase separation of phenyl- and naphthol-substituted Tiq analogs was accomplished by using polysaccharide-based CSPs [25]. Macrocyclic antibiotics [26, 27] and crown ether-based CSPs [28] were also applied for the enantioseparation of Tiq analogs.

Enantioselective retention and separation are usually influenced by temperature [29–33]. To determine the enthalpic and entropic contributions to the retention, van't Hoff plots are generally applied [34]. Without information concerning the phase ratio, the standard enthalpy and entropy cannot be determined [34], but if both enantiomers have access to the same stationary phase volume, the $\Delta(\Delta H°)$ and $\Delta(\Delta S°)$ values for the separated enantiomers can be determined from the relationship

$$\ln\alpha = -\frac{\Delta(\Delta H^\circ)}{RT} + \frac{\Delta(\Delta S^\circ)}{R} \quad (1)$$

where α is the selectivity factor ($\alpha = k_2/k_1$), $\Delta(\Delta H°)$ is the difference of standard enthalpy change, $\Delta(\Delta S°)$ is the difference of standard entropy change for the two enantiomers, R is the gas constant, and T is temperature in Kelvin.

The present paper first time describes HPLC methods for the enantioseparation of basic Tiq analogs (Fig. 1) on *Cinchona* alkaloid-based zwitterionic selectors (SOs), which also act as enantioselective cation exchangers (Fig. 2).

The effects of the mobile phase composition, the nature and concentrations of various mobile phase additives, the specific structural features of the Tiq analytes (selectands, SAs) and SOs, and temperature on the retention and stereoselectivity are discussed on the basis of the experimental data. Our objective was to elucidate the effects of structural changes in Tiq analogs on their chromatographic behavior on the ZWIX chiral columns. For the purposes of this study, the classical van't Hoff approach assuming only one site interaction was used. For a more realistic approach to the thermodynamic

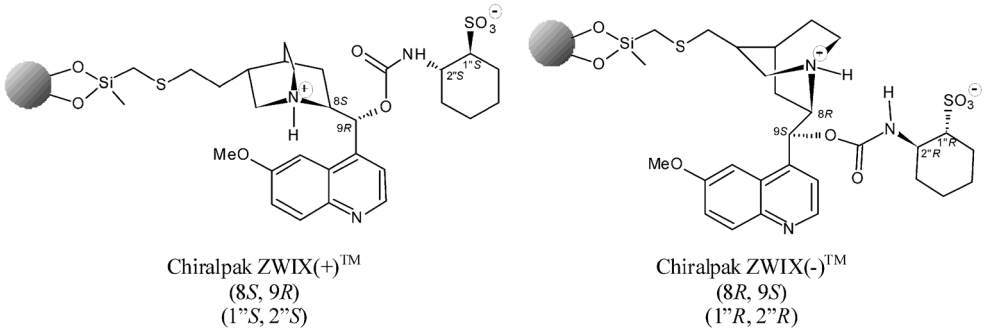

Fig. 2 Structures of *Cinchona* alkaloid-based CSPs

calculations, the contributions of enantioselective and nonselective sites should be distinguished. This can be achieved through the application of nonlinear characterization methods [35, 36]. The elution sequence was determined for analytes **2**, **8**, **9**, and **10**.

Materials and methods

Chemicals and reagents

(*S,R*)-**1**—(*S,R*)-**7** (Table 1) were synthesized by standard literature protocols, from the corresponding phenylethylamine, through acylation and then Bischler–Napieralski cyclization [37]. The dihydroisoquinolines obtained were reduced to tetrahydro derivatives with sodium borohydride [38]. (*R*)-**2** was prepared from racemic-**2** with (*R,R*)-dibenzoyltartaric acid. The racemic (*S,R*)-**8**, (*S,R*)-**9**, and (*S,R*)-**10** were obtained by known literature methods [36–40]. Calycotomine, (*S,R*)-**8**, was prepared from β-(3,4-dimethoxyphenyl)ethylamine, which was reacted with diethyl oxalate. The product amide was cyclized in a Bischler–Napieralski reaction and the resulting ethyl 6,7-dimethoxy-3,4-dihydroisoquinoline-1-carboxylate was reduced on Pt/C, followed by reduction with $LiAlH_4$ [38, 39]. Homocalycotomine, (*S,R*)-**9**, was prepared via the reaction of homoveratrylamine and formic acid. The resulting formamide was ring-closed in a Bischler–Napieralski reaction. The 6,7-dimethoxy-3,4-dihydroisoquinoline obtained was then transformed into an amino acid by reaction with malonic acid, and the product was reduced to the desired (*S,R*)-**9** with $LiAlH_4$ [39, 40]. (*S,R*)-1-(3-hydroxypropyl)-6,7-dimethoxy-Tiq, (*S,R*)-**10**, was prepared through the reaction of homoveratrylamine and γ-butyrolactone. The corresponding amide was cyclized in a Bischler–Napieralski reaction and the resulting 1-(3-hydroxypropyl)-6,7-dimethoxy-3,4-dihydroisoquinoline was reduced with sodium borohydride to furnish the desired (*S,R*)-**10** [41, 42]. The enantiomers of (*S*)-**8**, (*R*)-**9** and (*R*)-**10** were prepared through enzyme-catalyzed *O*-acylation of *N*-Boc-protected racemic **8**–**10** [41–43]. (*S,R*)-4-Chloro-*N*-methyl-2-Tiq-1-yl)aniline [(*S,R*)-**11**] was purchased from Sigma-Aldrich (St. Louis, MO, USA).

Acetonitrile (MeCN) and methanol (MeOH) of HPLC grade were purchased from VWR International (Arlington Heights, IL, USA), while NH_3, ethylamine (EA), diethylamine (DEA), triethylamine (TEA), propylamine (PRA), formic acid (FA), glacial acetic acid (AcOH), and

Table 1 Chromatographic parameters, retention factors (k), selectivity factor (α), resolution (R_S), and elution sequence of Tiq analogs on ZWIX(+)™ column

Compound	Eluent	k_1	k_2	α	R_S	Elution sequence
1	**a**	6.50	7.82	1.20	2.22	n.d.
	c	3.07	3.43	1.12	1.25	n.d.
2	**a**	8.02	9.99	1.25	4.17	*R*<*S*
	c	3.46	3.95	1.14	2.17	*R*<*S*
3	**a**	4.04	4.39	1.09	1.50	n.d.
	c	2.57	2.67	1.04	0.53	n.d.
4	**a**	6.25	6.53	1.04	0.87	n.d.
	c	3.18	3.42	1.08	1.27	n.d.
5	**a**	3.85	4.12	1.07	1.17	n.d.
	c	2.50	2.60	1.04	0.71	n.d.
6	**a**	5.93	6.10	1.03	0.53	n.d.
	c	3.11	3.14	1.01	<0.20	n.d.
7	**a**	7.14	7.21	1.01	<0.20	n.d.
	c	3.14	3.24	1.03	0.53	n.d.
8	**a**	5.51	5.96	1.08	0.40	*R*<*S*
	c	3.16	3.32	1.05	0.67	*R*<*S*
9	**a**	4.85	5.96	1.23	3.31	*R*<*S*
	c	2.81	3.05	1.09	1.45	*R*<*S*
10	**a**	5.33	5.74	1.08	1.29	*R*<*S*
	c	3.06	3.24	1.06	0.86	*R*<*S*
11	**a**	n.r.	n.r.	–	–	n.d.
	c	1.16	1.33	1.15	1.80	n.d.

Chromatographic conditions: column, Chiralpak ZWIX(+)™; mobile phase, **a**, MeOH/MeCN (25/75 *v/v*) containing 12.5 mM TEA and 25 mM AcOH; **c**, MeOH/MeCN (75/25 *v/v*) containing 12.5 mM TEA and 25 mM AcOH; flow rate, 0.6 ml min^{-1}; detection, 215 or 230 nm

n.d. not determined, *n.r.* no retardation

other reagents of analytical reagent grade were from Sigma-Aldrich. The Milli-Q water was further purified by filtration on a Millipore 0.45-μm filter, type HV (Molsheim, France).

Before use, all eluents were degassed in an ultrasonic bath, and gaseous helium was purged through them during the HPLC analyses. Stock solutions of analytes (1 mg ml^{-1}) were prepared by dissolution of the samples in MeOH.

Apparatus

Chromatographic measurements were carried out on a 1100 Series HPLC system from Agilent Technologies (Waldbronn, Germany), consisting of a solvent degasser, a pump, an autosampler, a column thermostat, and a multiwavelength UV–VIS detector. Data acquisition and analysis were performed with ChemStation chromatographic data software from Agilent Technologies. As alternative, a Waters HPLC system consisting of an M-600 low-pressure gradient pump, an M-2996 photodiode-array detector, and an Empower 2 Chromatography Manager data system (Waters Chromatography, Milford, MA, USA) equipped with a Rheodyne Model 7125 injector (Cotati, CA, USA) with a 20-μl loop was employed. A Spark Mistral column thermostat (Spark Holland, Emmen, The Netherlands) with a temperature adjustment precision of ±0.1 °C was used to thermostat the columns.

The Chiralpak ZWIX(+)™ and ZWIX(−)™ columns (150×3.0 mm I.D., 3-μm particle size) were gifts from Chiral Technologies Europe (Illkirch, France). As a void volume (t_0) marker, a methanolic solution of acetone was injected at each investigated temperature and eluent composition.

Results and discussion

Mobile phase selection

The zwitterionic ZWIX(+)™ and ZWIX(−)™ columns have been used for the enantiodiscrimination of hydroxy acids [44], small peptides [45, 46], chiral acids, and bases [47], and have previously mostly been applied for the resolution of diverse ampholytic non-cyclic and cyclic amino acids [48–54]. However, in view of the chemical nature and ampholytic property of the ZWIX selector, it can also be used as a chiral anion and cation exchanger. In the following, we concentrate on the latter use.

ZWIX(+)™ and ZWIX(−)™ columns are most frequently used with MeOH as protic polar bulk solvent (which can modify H-bonding interactions) and MeCN as an aprotic, but polar bulk solvent (which can support ion-pair formation, but interferes with π-π-type interactions), in combination with base and acid additives leading to the polar-ionic mobile phase mode, PIM. The effects of the composition of the bulk solvent on the chromatographic parameters in the case of Tiq analogs were investigated on ZWIX(+)™ and ZWIX(−)™ CSPs, which behave pseudo-enantiomerically. (Quinine and quinidine and their corresponding derivatives are under C_9 stereochemical control where they exhibit opposite configurations. Hence, the selectors applied in this study frequently reveal pseudoenantiomeric characteristic which is chromatographically materialized in reversed elution orders [55].) The chromatographic data determined for **8**, **9**, and **10** with mobile phase systems of MeOH/MeCN (75/25, 50/50, or 25/75 *v/v*) containing 25 mM AcOH and 12.5 mM TEA or 25 mM FA and 12.5 mM TEA, the acid-to-base ratio being maintained constant at 2:1, are depicted in Fig. 3a, b and are listed for the other analogs in Tables 1 and 2.

The retention of the Tiq analogs increased substantially with increasing MeCN content in the mobile phase, which is accompanied by two effects: the ionic interactions become stronger and the solvation effect may decrease. Furthermore, a marked increase in separation performance was observed at 75 % MeCN content. This observation is in contrast with the results obtained for α-amino acids, where the presence of a higher MeCN content usually led to decreases in enantioselectivity [48, 49], where as it is in accordance with the results obtained for secondary and β-amino acids, where increasing k, α, and R_S were found with increasing MeCN content [50–54]. These results indicate that the MeCN-to-MeOH ratio is a fine-tuning variable for optimization of the performance of the zwitterionic CSPs that we used as cation exchangers to resolve chiral bases.

The chargeable secondary amino group of the investigated Tiq analogs can be identified as the site of primary interaction, with the chiral sulfonic acid group (cation-exchanger site) of the SOs. The ionization state of the SO and SA as a function of the mobile phase composition will evidently influence the retention and enantioseparation, although the sulfonic acid group will be permanently charged as it is a strong acid. The effects of the ionization state of the SO, SA, and mobile phase were investigated on ZWIX(−)™ CSP for SAs **8**–**10**, with applying MeOH/MeCN (50/50 *v/v*) as bulk solvent containing 10, 25, or 50 mM AcOH and 5, 12.5, or 25 mM TEA (the same concentrations were used in the FA-TEA system; the acid-to-base ratio was kept constant at 2:1). The pK_a values of the secondary amino group within the Tiq and TEA and the carboxy group in FA and AcOH are ca. 9.1, 10.75, 3.75, and 4.76, respectively [56, 57]. The pK_a values of the quin uclidine nitrogen and of the sulfonic acid group of the SOs are ca. 9.8 and 1.0, respectively [58]. (It should be noted that pK_a values are defined for aqueous conditions; in pure organic media, they may shift considerably to higher values [59].) The results depicted in Fig. 4 show that a decrease of the amount of acid and base additives in the mobile phase (a decrease of the

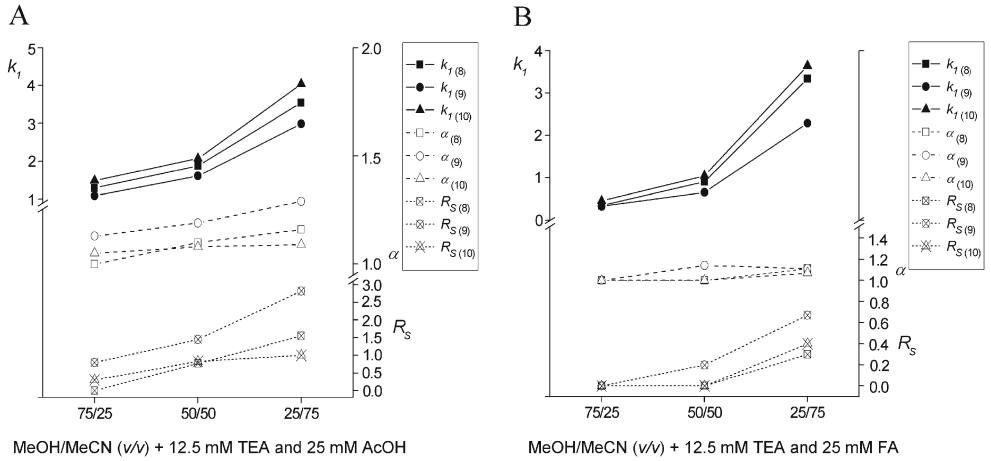

Fig. 3 Effects of the bulk solvent composition of the mobile phase on the chromatographic parameters, retention factor (k_1), selectivity factor (α), and resolution (R_S) of SAs **8**, **9**, and **10** on ZWIX(−)™ column. Chromatographic conditions: column, Chiralpak ZWIX(−)™; mobile phase, **a**, MeOH/MeCN (25/75 *v/v*) containing 12.5 mM TEA and 25 mM AcOH; **b**, MeOH/MeCN (50/50 *v/v*) containing 12.5 mM TEA and 25 mM AcOH; **c**, MeOH/MeCN (75/25 *v/v*) containing 12.5 mM TEA and 25 mM AcOH; **d**, MeOH/MeCN (25/75 *v/v*) containing 12.5 mM TEA and 25 mM FA; **e**, MeOH/MeCN (50/50 *v/v*) containing 12.5 mM TEA and 25 mM FA; **f**, MeOH/MeCN (75/25 *v/v*) containing 12.5 mM TEA and 25 mM FA; flow rate, 0.6 ml min^{-1}; detection, 230 and 258 nm

Table 2 Chromatographic parameters, retention factors (k), selectivity factor (α), resolution (R_S), and elution sequence of Tiq analogs on ZWIX(−)™ column

Compound	Eluent	k_1	k_2	α	R_S	Elution sequence
1	**a**	4.44	6.12	1.38	2.07	n.d.
	c	1.45	1.79	1.24	1.26	n.d.
2	**a**	6.73	9.99	1.48	3.10	*S*<*R*
	c	1.80	2.09	1.17	0.83	*S*<*R*
3	**a**	2.66	3.14	1.18	1.14	n.d.
	c	1.27	1.41	1.11	0.55	n.d.
4	**a**	5.18	6.30	1.22	1.53	n.d.
	c	2.04	2.51	1.23	1.50	n.d.
5	**a**	2.24	2.50	1.12	0.50	n.d.
	c	1.25	1.25	1.00	0.00	n.d.
6	**a**	2.24	2.50	1.12	0.50	n.d.
	c	1.56	1.56	1.00	0.00	n.d.
7	**a**	4.73	4.73	1.00	0.00	n.d.
	c	1.70	1.70	1.00	0.00	n.d.
8	**a**	3.55	4.13	1.16	1.55	*S*<*R*
	c	1.29	1.29	1.00	0.00	n.d.
9	**a**	2.99	3.85	1.29	2.82	*S*<*R*
	c	1.09	1.22	1.13	0.80	*S*<*R*
10	**a**	4.04	4.39	1.09	1.00	*S*<*R*
	c	1.49	1.56	1.05	0.30	*S*<*R*
11	**a**	n.r.	n.r.	–	–	n.d.
	c	0.61	0.72	1.19	1.00	n.d.

Chromatographic conditions: column, Chiralpak ZWIX(−)™; mobile phase, **a**, MeOH/MeCN (25/75 *v/v*) containing 12.5 mM TEA and 25 mM AcOH; **c**, MeOH/MeCN (75/25 *v/v*) containing 12.5 mM TEA and 25 mM AcOH; flow rate, 0.6 ml min^{-1}; detection, 215 or 230 nm

n.d. not determined, *n.r.* no retardation

"ionic strength") is accompanied by an increase in the extent of retention.

It is noteworthy that this increase was more pronounced with AcOH than with FA. Under slightly acidic mobile phase conditions, the Tiq moiety and TEA are in protonated form ("ammonium ion"), while the equimolar amounts of FA and AcOH are deprotonated. The excess of FA and AcOH is formally protonated, but can also act as a displacer in this form also. On increase of the salt concentration in the mobile phase, the increased amount of "ammonium ions" resulted in a decrease in retention, typically observed in ion-exchange chromatography and in accordance with the stoichiometric displacement model. FA is a stronger acid than AcOH, and its application led to a decreased retention. The effects of different strengths of FA and AcOH are seen in terms of retention, but as concerns the overall observed effect on retention, a smaller increase was observed for FA than in the case of AcOH. The different effect by AcOH and FA can be readily explained on the basis of their pK_a value and the dominant ion-exchange mechanism. As regards the change of enantioselectivity, the influence of the nature of the acidic additives was minor.

The nature of the amine component in the mobile phase influences the retention of SAs through their competition for the acidic sites of the SO. An amine added to the acidic mobile phase will be ionized (protonated) and may take part in a strong electrostatic interaction with the deprotonated sulfonic acid moiety of SO via displacement. Five different bases (NH_3, EA, DEA, TEA, and PRA; pK_a values of 9.25, 10.70, 10.84, 10.75, and 10.60, respectively) and two acids (FA and AcOH) were selected to study the effects of base and acid additives. The bases differed in the degree and nature of their alkyl substitution (lipophilicity), while the acids differed by

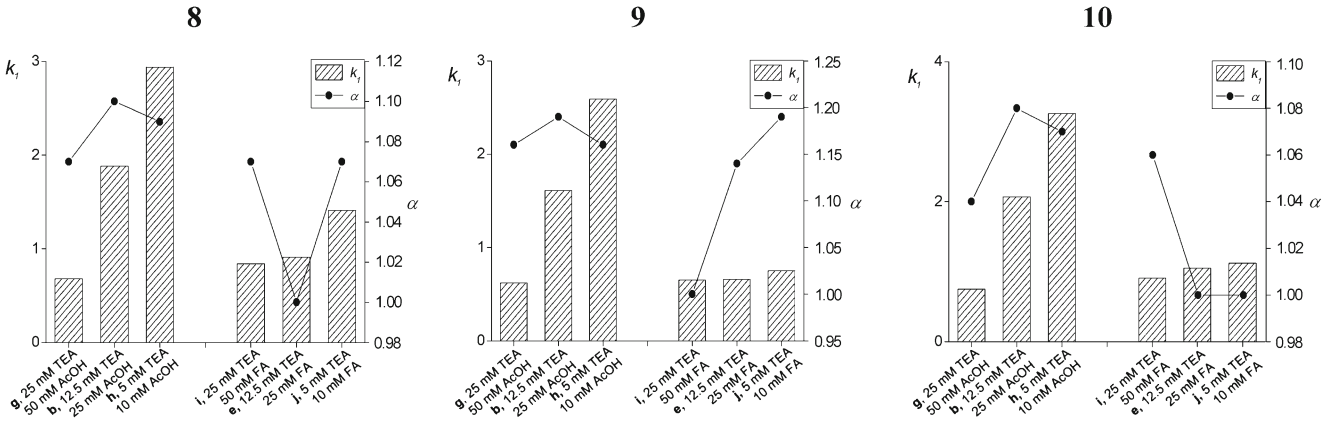

Fig. 4 Effects of the concentration of acid and base additives on the chromatographic parameters, retention factor (k_1), selectivity factor (α), and resolution (R_S) of SAs **8**, **9**, and **10** on the ZWIX(−)™ column. Chromatographic conditions: column, Chiralpak ZWIX(−)™; mobile phase, MeOH/MeCN (50/50 *v/v*) containing **g**, 25 mM TEA and 50 mM AcOH; **b**, 12.5 mM TEA and 25 mM AcOH; **h**, 5 mM TEA and 10 mM AcOH; **i**, 25 mM TEA and 50 mM FA; **e**, 12.5 mM TEA and 25 mM FA; **j**, 5 mM TEA and 10 mM FA; flow rate, 0.6 ml min^{-1}; detection, 230 and 258 nm

one methylene group. Figure 5 illustrates the chromatographic parameters for SA **8** on ZWIX(+)™ and ZWIX(−)™ with a mobile phase of MeOH/MeCN (50/50 *v/v*) containing 12.5 mM base and 25 mM acid.

In general, the more bulky and hydrophobic triethylammonium ion ensured the largest retention, and the smallest ammonium ion the lowest retention [an exception was eluent **e** on ZWIX(−)™], although the pK_a values differ by more than 1 unit. If the competing ionic interactions in the mobile and stationary phases are taken into account, the more polar and smaller ammonium ion can form more stable complexes than the protonated Tiq moiety with the cationic binding site of the SO, ensuring low retention, while the complex formation of the triethylammonium ion with the SO is probably less favorable. However, it is worthy of mention that some of the amine additives (NH_3 and TEA) used in the study are characterized by a different ability to participate in H-bond interactions influencing the retention behavior. The slight changes in α observed with variation of the nature of the amines (and also with acids) reveal a moderate effect on the overall selectivity. However, SA **8** was not separable on ZWIX(−)™ with the application of FA as additive (α=1; Fig. 5). In most cases, the resolution was larger when DEA or TEA was applied as compared with ammonia, EA, or PRA, independently of the nature of the acid used. In a discussion of these observations, the ionic radius of the solvated ionic species should also be considered, leading to the assumption that the electrostatic interaction responsible for retention is stronger overall for a smaller counter ion.

From the aspect of the chromatographic performance of the two investigated CSPs, it should be mentioned that use of the ZWIX(−)™ column in most cases led to lower retention times

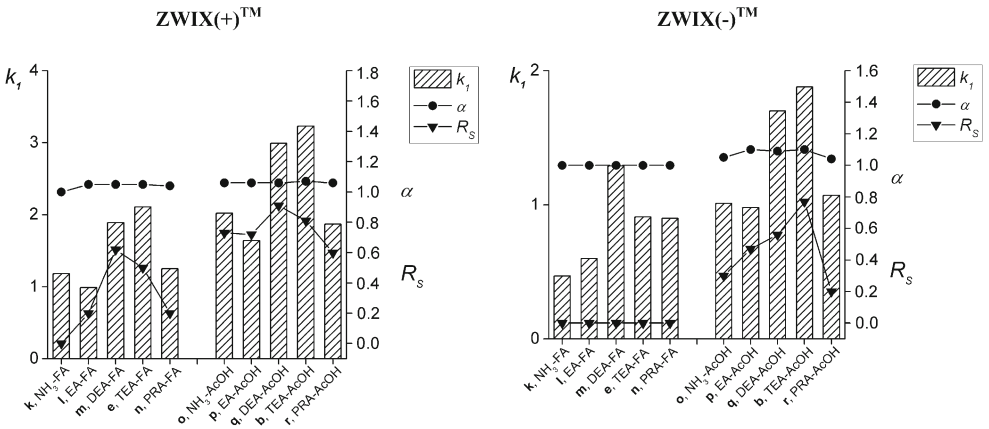

Fig. 5 Effects of nature of acid and base additives on the chromatographic parameters, retention factor (k_1), selectivity factor (α), and resolution (R_S) of **8** on the ZWIX(+)™ and ZWIX(−)™ columns. Chromatographic conditions: column, ZWIX(+)™ or ZWIX(−)™; mobile phase, MeOH/MeCN (50/50 *v/v*) containing **k**, 12.5 mM NH_3 and 25 mM FA; **l**, 12.5 mM EA and 25 mM FA; **m**, 12.5 mM DEA and 25 mM FA; **e**, 12.5 mM TEA and 25 mM FA; **n**, 12.5 mM PRA and 25 mM FA; **o**, 12.5 mM NH_3 and 25 mM AcOH; **p**, 12.5 mM EA and 25 mM AcOH; **q**, 12.5 mM DEA and 25 mM AcOH; **b**, 12.5 mM TEA and 25 mM AcOH; **r**, 12.5 mM PRA and 25 mM AcOH; flow rate, 0.6 ml min^{-1}; detection, 230 and 258 nm

and higher enantioselectivities (Tables 1 and 2). Similar phenomena were observed earlier for various unusual α- and β-amino acids [50–54].

Structure–retention (selectivity) relationships

The sterically demanding structures of the constrained SAs (Fig. 1) influence the retention and the chiral recognition. Tables 1 and 2 report the k and α values observed with the most frequently applied mobile phases on the ZWIX(+)™ and ZWIX(−)™ columns in this study. At the same mobile phase composition, the methoxy substitution in **2** as compared with **1** resulted in higher k and α values, similarly as in the case of **6** and **7**, but **7** was not separable on ZWIX(−)™. The increased π-basicity and molecular size of the analytes, together with a possible H-bond interaction of the methoxy group with the SO, may explain the increased retention and selectivity. For analytes **2**–**5**, k_1 varied with the length of the alkyl chain in the molecule; increasing chain length and a bulkier molecular structure probably sterically hinder the stabilization of the SO-SA complex, and therefore k_1 decreased in parallel with the selectivity. Comparison of the chromatographic behavior of **8**–**10** with that of **2** reveals that hydroxyalkyl substitution, especially in eluent **a**, weakens the SA-SO complexation, resulting in decreases in both k and α. The chain length of the hydroxyalkyl group has a small effect on the chromatographic behavior, but **9** undergoes the best steric fit to the SO, resulting in higher k and α values on both CSPs.

Elution sequence

The chiral SOs of Chiralpak ZWIX(+)™ and ZWIX(−)™ CSPs are actually diastereomeric to each other (Fig. 2), but in most cases behave like pseudo-enantiomers [48, 49]. As a consequence, on change from the quinine-based CSP [ZWIX(+)™] to the quinidine-based CSP [ZWIX(−)™], reversal of the elution sequence of Tiq analogs may be expected. In several cases, it was in fact observed (Tables 1 and 2).

On ZWIX(+)™, analytes with *S* configuration are more strongly retained, obviously form more stable complexes within the binding pocket associated with the 8*S* and 9*R*-configurated chiral centers of the *Cinchona*-based backbone. For ZWIX(−)™, the opposite is the case, the more strongly retained enantiomers have the *R* configuration, which is an indication that the change in the configuration of 8 and 9 chiral

Table 3 Thermodynamic parameters, $\Delta(\Delta H°)$, $\Delta(\Delta S°)$, $T\times\Delta(\Delta S°)$, $\Delta(\Delta G°)$, and correlation coefficients (R^2) of Tiq analogs on ZWIX(+)™ and ZWIX(−)™ columns

Analyte	Column	$-\Delta(\Delta H°)$ (kJ mol^{-1})	$-\Delta(\Delta S°)$ (J mol^{-1} K^{-1})	Corr. coeff. (R^2)	$-T\times\Delta(\Delta S°)_{29\ K}$ (kJ mol^{-1})	$-\Delta(\Delta G°)_{298\ K}$ (kJ mol^{-1})
1	ZWIX(+)™	1.9	5.2	0.9942	1.5	0.4
	ZWIX(−)™	2.4	5.6	0.9958	1.7	0.7
2	ZWIX(+)™	2.0	5.2	0.9927	1.5	0.5
	ZWIX(−)™	3.0	7.2	0.9993	2.2	0.8
5	ZWIX(+)™[a]	0.1	<<0.1	0.9971	<<0.1	0.1
	ZWIX(+)™[b]	1.2	3.6	0.9963	1.1	0.1
	ZWIX(−)™[a]	−0.3	−1.7	0.9996	−0.5	0.2
	ZWIX(−)™[b]	0.3	0.2	0.9995	0.1	0.2
6	ZWIX(+)™[a]	−0.6	−2.1	0.9901	−0.6	<<0.1
	ZWIX(+)™[b]	1.0	3.1	0.9968	0.9	0.1
	ZWIX(−)™	–	–	–	–	
7	ZWIX(+)™[a]	<<0.1	−0.3	0.9954	−0.1	0.1
	ZWIX(+)™[b]	0.4	1.1	0.9926	0.1	0.3
	ZWIX(−)™	–	–	–	–	–
8	ZWIX(+)™	0.4	0.8	0.9991	0.2	0.2
	ZWIX(−)™	0.8	1.8	0.9989	0.5	0.3
9	ZWIX(+)™	1.0	2.1	0.9994	0.6	0.4
	ZWIX(−)™	1.5	3.4	0.9997	1.0	0.5
10	ZWIX(+)™	0.7	2.0	0.9994	0.6	0.1
	ZWIX(−)™	0.8	1.9	0.9994	0.6	0.2

Chromatographic conditions: column, Chiralpak ZWIX(+)™ and ZWIX(−)™; mobile phase, **b**, MeOH/MeCN (50/50 *v/v*) containing 12.5 mM TEA and 25 mM AcOH; flow rate, 0.6 ml min^{-1}; detection, 215 or 230 nm; R^2, correlation coefficient of van't Hoff plot, ln $\alpha-1/T$ curves

[a] Temperature range: 10–30 °C

[b] Temperature range 30–50 °C

centers of the SO leads to a change in the enantiorecognition process.

Effects of temperature and thermodynamic parameters

The effects of temperature on the chromatographic parameters for **1**, **2**, and **5**–**10** were studied on ZWIX(+)™ and ZWIX(−)™ over the temperature range 10–50 °C. Experimental data on both columns with a mobile phase of MeOH/MeCN (50/50 *v/v*) containing 25 mM AcOH and 12.5 mM TEA are presented in Supplementary Material Tables S1 and S2.

In several cases, the *k* values on ZWIX(+)™ decreased with increasing temperature, as expected, but for **1**, **2**, **5**, **7**, and **9** in the range 10–30 °C, *k* increased with increasing temperature, which is unusual. This quite unique behavior was observed on the ZWIX(−)™ column throughout the entire temperature range (10–50 °C): with increasing temperature, *k* increased, but α decreased (the only exception was **5**). Adlof and List [60], Wu et al. [61], and Yogo et al. [62] earlier registered increasing *k* and α values with increasing temperature for non-chiral separations, and Matarashvili et al. [63] and Ilisz et al. [52–54] recently described the same phenomenon for chiral separations. Our observations relate mainly to the quinidine-based ZWIX(−)™ column [49–51]. It should be pointed out again that the configurations of the selectors of the ZWIX(+)™ and ZWIX(−)™ columns (Fig. 2) are not enantiomeric to each other, as the three chiral centers of the quinuclidine ring (1, 3, and 4) are identical in both chiral selectors, whereas the other four chiral centers (8, 9, 1″, and 2″) switch consequently. This certainly has an effect on the accessibility of specific binding sites and their solvation. Further studies are required for a better understanding of this phenomenon.

The changes observed in selectivity with temperature were inconsistent. As usual, α (and R_S; Tables S1 and S2) decreased with increasing temperature, but for **6** and **7** on ZWIX(+)™ and for **5** on ZWIX(−)™ in the temperature range 10–30 °C, α increased with increasing temperature.

Since the effects of temperature on enantiomer separation are complex, thermodynamic parameters were established on the basis of the chromatographic data

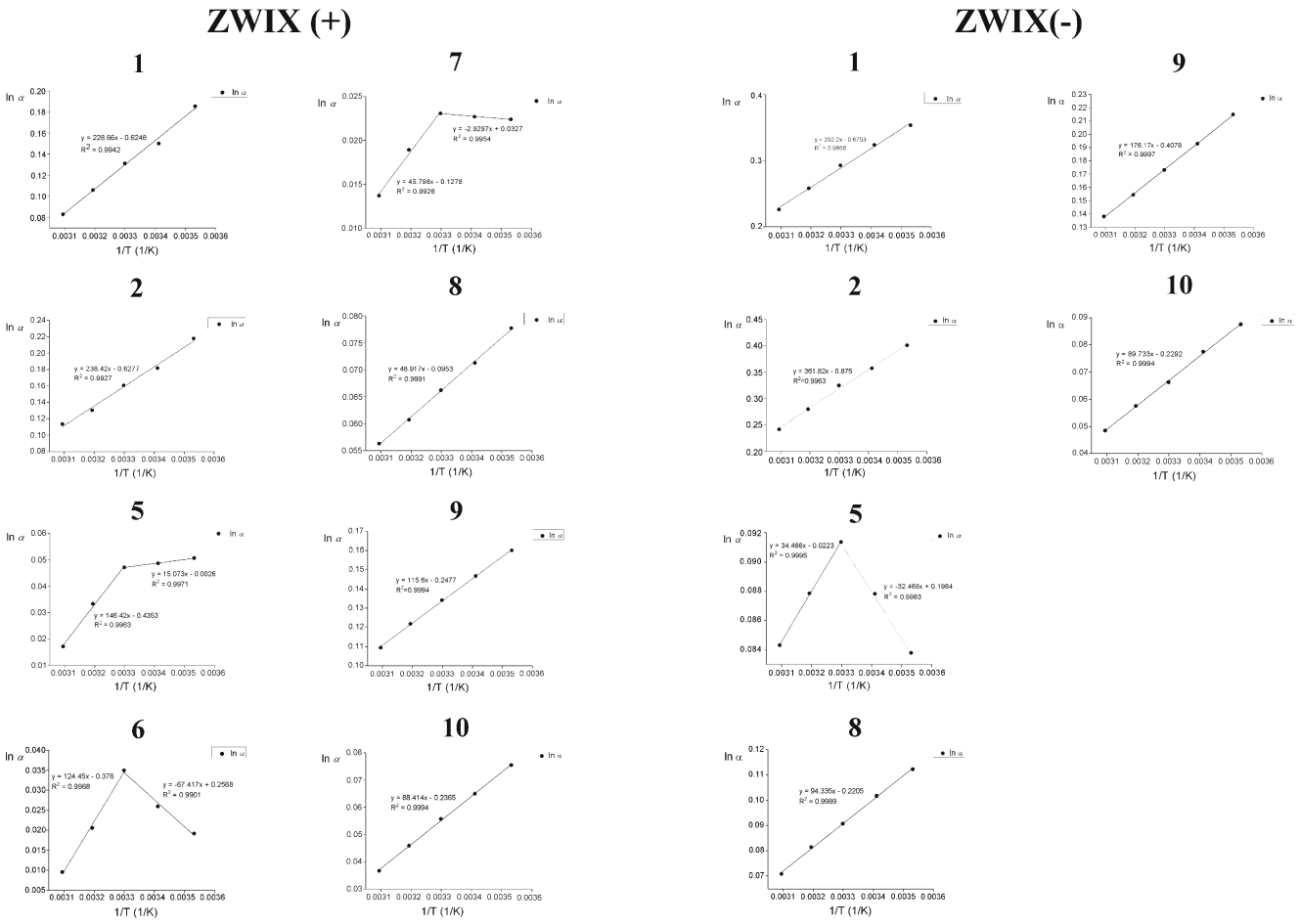

Fig. 6 van't Hoff plots for the separation factor (α) of **1**, **2**, and **5**–**10** on ZWIX(+)™ and ZWIX(−)™ columns. Chromatographic conditions: column, ZWIX(+)™ or ZWIX(−)™; mobile phase, **b**, MeOH/MeCN (50/50 *v/v*) containing 12.5 mM TEA and 25 mM AcOH; flow rate 0.6 ml min^{-1}; detection 230 and 258 nm

through the application of van't Hoff plots [Eq. (1)]. The differences in the changes in standard enthalpy and entropy, calculated from the ln α vs *1/T* curves, $-\Delta(\Delta H°)$ and $-\Delta(\Delta S°)$, are presented in Table 3.

The $\Delta(\Delta H°)$ values ranged from −3.0 to 0.6 kJ mol^{-1} and were slightly more negative on ZWIX(−)™ than on ZWIX(+)™ [exceptions were **5** and **8**; **6** and **7** were not separable on ZWIX(−)™ under the condition applied in the thermodynamic study]. The trends in the change in $\Delta(\Delta S°)$ and $\Delta(\Delta H°)$ were similar. Under the conditions where $\Delta(\Delta H°)$ has negative values, $\Delta(\Delta S°)$ was also negative, and the largest positive $\Delta(\Delta H°)$ was accompanied by the largest positive $\Delta(\Delta S°)$. The interactions of **1** and **2** with ZWIX(+)™ and ZWIX(−)™ were characterized by the highest $-\Delta(\Delta H°)$ and $-\Delta(\Delta S°)$ values.

As shown in Fig. 6, linear fits could generally be plotted, but for **5**, **6**, and **7** on ZWIX(+)™ and for **5** on ZWIX(−)™, the ln α vs *1/T* plots could be divided into two linear regions, which means that the linear van't Hoff plots reflect different overall binding situations in limited temperature ranges. (In these cases, in Table 3 presents values calculated for the two temperature ranges independently.)

In the temperature range 10–30 °C for **5** on ZWIX(−)™ and for **6** and **7** on ZWIX(+)™, the separations exhibited relatively small $-\Delta(\Delta H°)$ and larger $-T\times\Delta(\Delta S°)$ values, i.e., a larger contribution of entropy to the enantioseparation is observed in this temperature region.

The thermodynamic parameter $-\Delta(\Delta G°)_{298}$ suggests that, both on ZWIX(+)™ and on ZWIX(−)™ for **1** and **2** in mobile phase **b**, the binding to the SO was induced more efficiently,

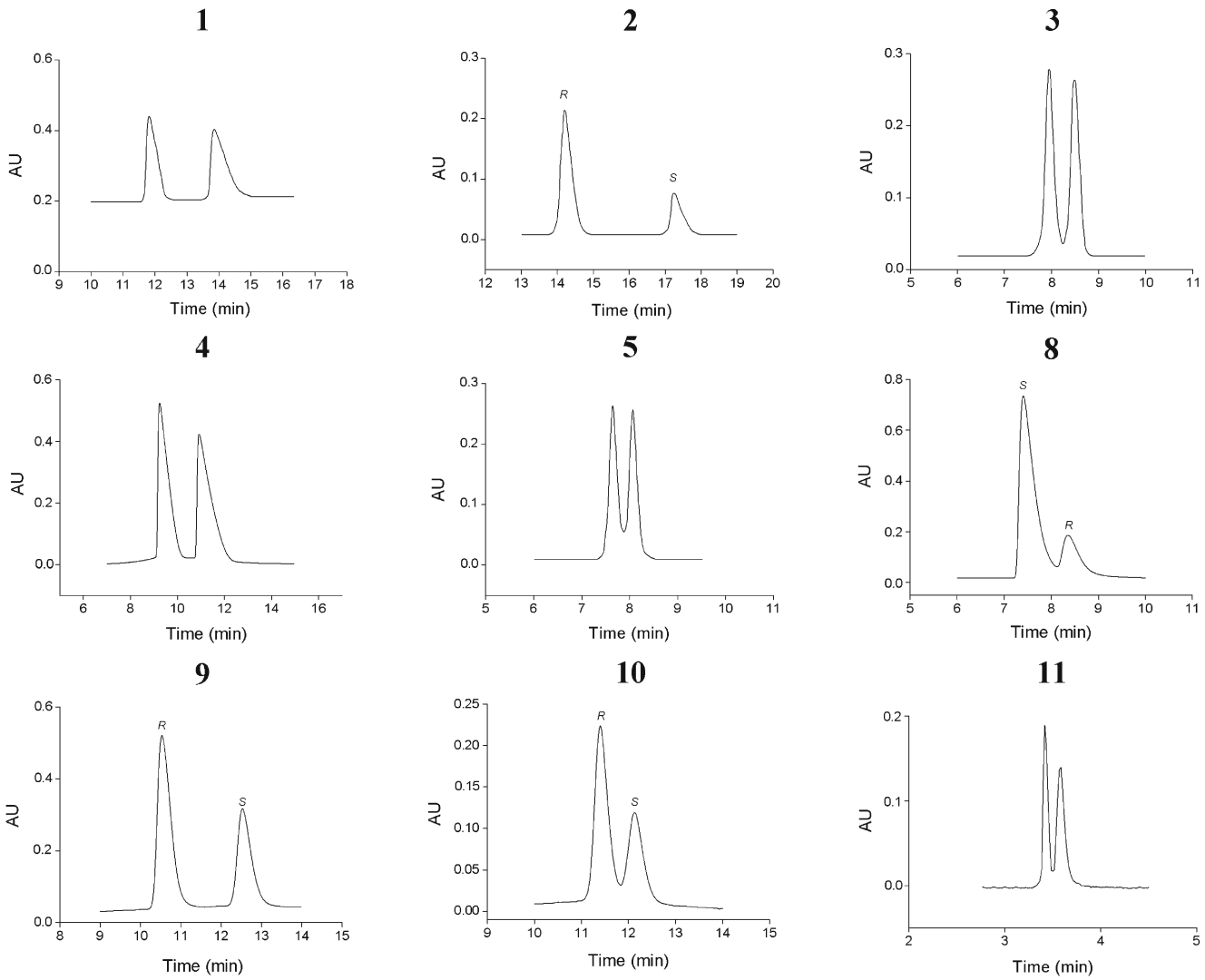

Fig. 7 Selected chromatograms of Tiq analogs. Chromatographic conditions: column, ZWIX(+)™ for **1**–**3**, **5**, and **9**–**11**, and ZWIX(−)™ for **4** and **8**; mobile phase, for **1**–**4** and **8**–**10**, MeOH/MeCN (25/75 *v/v*) containing 12.5 mM TEA and 25 mM AcOH, for **11** MeOH/MeCN (75/25 *v/v*) containing 12.5 mM TEA and 25 mM AcOH; flow rate, 0.6 ml min^{-1}; detection, 230 nm and 258 nm; temperature, 25 °C; the peaks in the chromatograms for **2** and **8**–**10** are those of mixtures of the racemic compound and enantiomer

as reflected by the largest $-\Delta(\Delta G°)$ values. Apart from a few exceptions (in the temperature range 10–30 °C), it can be concluded from the $-\Delta(\Delta H°)$ and $-T\Delta(\Delta S°)$ data for all the SAs that the enantioresolution is predominantly enthalpically driven, and the selectivity increases with decreasing temperature. The $-\Delta(\Delta G°)_{298}$ values were generally slightly larger on ZWIX(−)™ than on ZWIX(+)™, which is in accordance with results obtained for unusual α- and β-amino acids [50–54].

Selected chromatograms of Tiq analogs are depicted in Fig. 7.

Conclusions

The enantiomers of Tiq analogs representing a group of chiral basic compounds were separated on Chiralpak ZWIX(+)™ and ZWIX(−)™ columns, containing quinine- or quinidine-based zwitterionic selectors. The chromatographic parameters depended on the mobile phase composition, the nature and concentrations of the mobile phase additives, and temperature. Baseline resolution was achieved in all cases, and the newly commercialized zwitterionic CSPs therefore also behave as chiral cation exchangers. The elution sequence was determined in some cases and revealed that these CSPs behave pseudo-enantiomerically to each other, leading to a reversal of the elution sequence on the quinine-based ZWIX(+)™ and on the quinidine-based ZWIX(−)™ SOs. This is advantageous from the aspect of the chiral separation of minor components in the presence of a major one.

Results obtained in this study contribute to shed light on the enantiodiscrimination process observed with zwitterionic selectors and serve valuable data for the enantioseparation of biologically important Tiq analogs.

Acknowledgments This work was supported by OTKA grant T 108847. A.P. is grateful to Pilar Franco for the ZWIX(+)™ and ZWIX(−)™ columns.

References

1. Miyazaki M, Ando N, Sugai K, Seito Y, Fukuoka H, Kanemitsu T, Nagata K, Odanaka Y, Nakamura KT, Itoh T (2011) Catalytic asymmetric allylation of 3,4-dihydroisoquinolines and its application to the synthesis of isoquinoline alkaloids. J Org Chem 76:534–542
2. Chrzanowska M, Rozwadowska MD (2004) Asymmetric synthesis of isoquinoline alkaloids. Chem Rev 104:3341–3370
3. Kashiwada Y, Aoshima A, Ikeshiro Y, Chen Y-P, Furukawa H, Itoigawa M, Fujioka T, Mihashi K, Cosentino LM, Morris-Natschke SL, Lee K-H (2005) Anti-HIV benzylisoquinoline alkaloids and flavonoids from the leaves of *Nelumbo nucifera*, and structure–activity correlations with related alkaloids. Bioorg Med Chem 13:443–448
4. Nikulin VI, Rakov IM, De Los Angeles JE, Mehta RC, Boyd LY, Feller DR, Miller DD (2006) 1-Benzyl-1,2,3,4-tetrahydroisoquinoline-6,7-diols as novel affinity and photoaffinity probes for β-adrenoceptor subtypes. Bioorg Med Chem 14:1684–1697
5. Naoi M, Maruyama W, Dostert P, Kohda K, Kaiya T (1996) Cloning of the 3′ end of rat *bax*-α and corresponding developmental down-regulation in differentiating primary, cultured oligodendrocytes. Neurosci Lett 212:183–186
6. Taniyama D, Hasegawa M, Tomioka T (1999) A facile asymmetric synthesis of 1-substituted tetrahydroisoquinoline based on a chiral ligand-mediated addition of organolithium to imine. Tetrahedron Asymmetry 10:221–223
7. Tietze LF, Rackelmann N, Müller I (2004) Enantioselective total syntheses of the Ipecacuanha alkaloid emetine, the Alangium alkaloid tubulosine and a novel benzoquinolizidine alkaloid by using a domino process. Chem Eur J 10:2722–2731
8. Zhang Q, Tu G, Zhao Y, Cheng T (2002) Novel bioactive isoquinoline alkaloids from *Carduus crispus*. Tetrahedron 58: 6795–6798
9. Haber H, Henklein P, Georgi M, Melzig MF (1995) Resolution of catecholic tetrahydroisoquinoline enantiomers and the determination of *R*- and *S*-salsolinol in biological samples by gas chromatography–mass spectrometry. J Chromatogr B 672:179–187
10. Musshoff F, Schmidt P, Dettmeyer R, Priemer F, Jachau K, Madea B (2000) Determination of dopamine and dopamine-derived (*R*)-/(*S*)-salsolinol and norsalsolinol in various human brain areas using solid-phase extraction and gas chromatography/mass spectrometry. Forensic Sci Int 113:359–366
11. Péter A, Péter M, Ilisz I, Fülöp F (2005) Comparison of column performances in direct high-performance liquid chromatographic enantioseparation of 1- or 3-methyl-substituted tetrahydroisoquinoline analogs. Application of direct and indirect methods. Biomed Chromatogr 19:459–465
12. Deng YL, Maruyama W, Kawai M, Dostert P, Yamamura H, Takahashi T, Naoi M (1997) Assay for the (*R*)- and (*S*)-enantiomers of salsolinols in biological samples and foods with ion-pair high-performance liquid chromatography using β-cyclodextrin as a chiral mobile phase additive. J Chromatogr B 689:313–320
13. McMurtrey K, Strawbridge C, McCoy J (2000) HPLC resolution of the enantiomers of dihydroxyphenylalanine and selected salsolinol derivatives using sulfated β-cyclodextrin. Enantiomer 5:377–383
14. DeCuypere M, Lu Y, Miller DD, LeDoux MS (2008) Regional distribution of tetrahydroisoquinoline derivatives in rodent, human, and Parkinson's disease brain. J Neurochem 107:1398–1413
15. Zhao SL, Shen JS (2006) Enantiomeric separation and determination of R, S-salsolinol by capillary electrophoresis. Chin J Chem 24:439–441
16. Quan Z, Song Y, Peters G, Shenwu M, Sheng Y, Hwang H-M, Liu Y-M (2005) Chiral CE separation of dopamine-derived neurotoxins. Anal Sci 21:115–119
17. Quan Z, Song Y, Saulsberry A, Sheng YH, Liu YM (2005) Capillary electrophoresis for diastereomers of (R, S)-tetrahydroisoquinoline-3-carboxylic acid derivatized with (R)-4-nitro-7-(3-aminopyrrolidin-1-yl)-2,1,3-benzoxadiazole. J Chromatogr Sci 43:121–125
18. Huang MJ, Quan Z, Liu YM (2009) Computational modeling of inclusion complexes of β-cyclodextrin with enantiomers of salsolinol, *N*-methyl-salsolinol and 1-benzyl-tetrahydroisoquinoline. Int J Quantum Chem 109:81–90
19. Liu YM, Gordon P, Green S, Sweedler JV (2000) Determination of salsolinol enantiomers by gas chromatography–mass spectrometry with cyclodextrin chiral columns. Anal Chim Acta 420:81–88
20. Deng Y, Maruyama W, Dostert P, Takahashi T, Kawai M, Naoi M (1995) Determination of the (*R*)-enantiomers and (*S*)-enantiomers of salsolinol and *N*-methylsalsolinol by use of a chiral high-performance liquid-chromatographic column. J Chromatogr B 670:47–54

21. Rommelspacher H, Baum SS, Dufeu P, Schmidt LG (1995) Determination of (*R*)- and (*S*)-salsolinol sulfate and dopamine sulfate levels in plasma of nonalcoholics and alcoholics. Alcohol 12:309–315
22. Stammel W, Woesle B, Thomas H (1995) Enantiomeric separation of tetrahydroisoquinoline alkaloids by high-performance liquid chromatography with β-cyclodextrin as chiral selector. Chirality 7:10–19
23. Zhang W, Wan FL, Xie YF, Gu J, Wang J, Yamamoto K, Jin LT (2004) Amperometric determination of (*R*)-salsolinol, (*R*)-*N*-methylsalsolinol and monoamine neurotransmitters with liquid chromatography using functionalized multi-wall carbon nanotube modified electrode in Parkinson's patients' cerebrospinal fluid. Anal Chim Acta 512:207–214
24. de los Angeles Juricic M, Berrios-Carcamo PB, Acevedo ML, Israel Y, Almodovar I, Cassels BK (2012) Salsolinol and isosalsolinol: condensation products of acetaldehyde and dopamine. Separation of their enantiomers in the presence of a large excess of dopamine. J Pharm Biomed Anal 63:170–174
25. Ilisz I, Gecse Z, Szatmári I, Fülöp F, Péter A (2014) High performance liquid chromatographic enantioseparation of naphthol-substituted tetrahydroisoquinolines on polysaccharide-based chiral stationary phases. Biomed Chromatogr. doi:10.1002/bmc.3002
26. Péter A, Vékes E, Armstrong DW (2002) Effects of temperature on retention of chiral compounds on a ristocetin A chiral stationary phase. J Chromatogr A 958:89–107
27. Péter A, Török G, Armstrong DW, Tóth G, Tourwe D (2000) High-performance liquid chromatographic separation of enantiomers of synthetic amino acids on a ristocetin A chiral stationary phase. J Chromatogr A 904:1–15
28. Lee A, Choi HJ, Jin KB, Hyun MH (2011) Liquid chromatographic resolution of 1-aryl-1,2,3,4-tetrahydroisoquinolines on a chiral stationary phase based on (+)-(18-crown-6)-2,3,11,12-tetracarboxylic acid. J Chromatogr A 1218:4071–4076
29. Götmar G, Fornstedt T, Guiochon G (2000) Retention mechanism of β-blockers on an immobilized cellulase. Relative importance of the hydrophobic and ionic contributions to their enantioselective and nonselective interactions. Anal Chem 72:3908–3915
30. Cavazzini A, Nadalini G, Dondi F, Gasparrini F, Ciogli A, Villani C (2004) Study of mechanisms of chiral discrimination of amino acids and their derivatives on a teicoplanin-based chiral stationary phase. J Chromatogr A 1031:143–158
31. Fornstedt T, Sajonz P, Guichon G (1998) A closer study of chiral retention mechanisms. Chirality 10:375–381
32. Peyrin E, Guillaume YC, Guinchard C (1997) Interactions between dansyl amino acids and human serum albumin using high-performance liquid chromatography: mobile phase pH and temperature considerations. Anal Chem 69:4979–4984
33. Castells CB, Carr RW (2000) A study of the thermodynamics and influence of temperature on chiral high-performance liquid chromatographic separations using cellulose-*tris*-(3,5-dimethylphenylcarbamate) coated zirconia stationary phases. Chromatographia 52:535–542
34. Chester TL, Coym JW (2003) Effect of phase ratio on van't Hoff analysis in reversed-phase liquid chromatography, and phase-ratio-independent estimation of transfer enthalpy. J Chromatogr A 1003: 101–111
35. Samuelsson J, Arnell R, Fornstedt T (2009) Potential of adsorption isotherm measurements for closer elucidating of binding in chiral liquid chromatographic phase systems. J Sep Sci 32:1491–1506
36. Fornstedt T (2010) Chracterization of adsorption process in analytical liquid–solid chromatography. J Chromatogr A 1217:792–812
37. Sotomayor N, Dominguez E, Lete E (1996) Bischler-Napieralski cyclization-N/C-alkylation sequences for the construction of isoquinoline alkaloids. Synthesis of protoberberines and benzo[c] phenanthridines via C-2′-functionalized 3-arylisoquinolines. J Org Chem 61:4062–4072
38. Zalán Z, Hetényi A, Lázár L, Fülöp F (2005) Substituent effects in the ring-chain tautomerism of 4-aryl-1,3,4,6,7,11b-hexahydro-2*H*-pyrimido[6,1-*a*]isoquinolines. Tetrahedron 61:5287–5295
39. Fülöp F, Forró E, Martinek T, Günther G, Sillanpää R (2000) Synthesis and stereochemistry of 1,3,2-oxazaphosphorino [4,3-a]isoquinolines. J Mol Struct 554:119–125
40. Campbell JA, Lee WK, Rapoport H (1995) Chirospecific syntheses of precursors of cyclopentane and cyclopentene carbocyclic nucleosides by [3+3]-coupling and transannular alkylation. J Org Chem 60: 4602–4616
41. Schönstein L, Forró E, Fülöp F (2013) Continuous-flow enzymatic resolution strategy for the acylation of amino alcohols with a remote stereogenic centre: synthesis of calycotomine enantiomers. Tetrahedron Asymmetry 24:202–206
42. Schönstein L, Forró E, Fülöp F (2013) Enzymatic reactions for the preparation of homocalycotomine enantiomers. Tetrahedron Asymmetry 24:1059–1062
43. Forró E, Schönstein L, Fülöp F (2011) Total synthesis of crispine A enantiomers through a Burkholderia cepacia lipase-catalysed kinetic resolution. Tetrahedron Asymmetry 22:1255–1260
44. Ianni F, Pataj Z, Gross H, Sardella R, Natalini B, Lindner W, Lämmerhofer M (2014) Direct enantioseparation of underivatized aliphatic 3-hydroxyalkanoic acids with a quinine-based zwitterionic chiral stationary phase. J Chromatogr A. doi:10.1016/j.chroma.2014.03.060
45. Wernisch S, Lindner W (2012) Versatility of cinchona-based zwitterionic chiral stationary phases: enantiomer and diastereomer separations of non-protected oligopeptides utilizing a multimodal chiral recognition mechanism. J Chromatogr A 1269: 297–307
46. Wernisch S, Pell R, Lindner W (2012) Increments to chiral recognition facilitating enantiomer separations of chiral acids, bases, and ampholytes using *Cinchona*-based zwitterion exchanger chiral stationary phases. J Sep Sci 35:1560–1572
47. Hoffmann CV, Pell R, Lämmerhofer M, Lindner W (2008) Synergistic effects on enantioselectivity of zwitterionic chiral stationary phases for separations of chiral acids, bases, and amino acids by HPLC. Anal Chem 80:8780–8789
48. Hoffmann CV, Reischl R, Maier NM, Lämmerhofer M, Lindner W (2009) Investigations of mobile phase contributions to enantioselectice anion- and zwitterion-exchange modes on quinine-based zwitterionic chiral stationary phases. J Chromatogr A 1216: 1157–1166
49. Pell R, Sic S, Lindner W (2012) Mechanistic investigations of cinchona alkaloid-based zwitterionic chiral stationary phases. J Chromatogr A 1269:287–296
50. Ilisz I, Grecsó N, Aranyi A, Suchotin P, Tymecka D, Wilenska B, Misicka A, Fülöp F, Lindner W, Péter A (2014) Enantioseparation of β^2-amino acids on cinchona alkaloid-based zwitterionic chiral stationary phases. Structural and temperature effects. J Chromatogr A 1334:44–54
51. Pataj Z, Ilisz I, Gecse Z, Szakonyi Z, Fülöp F, Lindner W, Péter A (2014) Effect of mobile phase composition on the liquid chromatographic enantioseparation of bulky monoterpene-based β-amino acids applying chiral stationary phases based on *Cinchona* alkaloid. J Sep Sci. doi:10.1002/jssc.20140078
52. Ilisz I, Pataj Z, Gecse Z, Szakonyi Z, Fülöp F, Lindner W, Péter A (2014) Unusual temperature-induced retention behavior of constrained β-amino acid enantiomers on the zwitterionic chiral stationary phases ZWIX(+)^{TM} and ZWIX(−)^{TM}. Chirality. doi:10.1002/chir.22333
53. Ilisz I, Gecse Z, Pataj Z, Fülöp F, Tóth G, Lindner W, Péter A (2014) Direct high-performance liquid chromatographic enantioseparation of secondary amino acids on *Cinchona* alkaloid-based chiral zwitterionic stationary phases. Unusual temperature behavior. J Chromatogr A (under revision)

54. Ilisz I, Grecsó N, Palkó M, Fülöp F, Lindner W, Péter A (2014) Structural and temperature effect on enantiomeric separation of bicyclo[222]octane based 3-amino-2-carboxylic acids on *Cinchona* alkaloid-based chiral stationary phases. J Pharm Biomed Anal 98: 130–139
55. Lämmerhofer M (2010) Chiral recognition by enantioselective liquid chromatography: mechanisms and modern chiral stationary phases. J Chromatogr A 1217:814–856
56. Zhang S (2012) A reliable and efficient first principles-based method for predicting pK_a values. 4. Organic bases. J Comput Chem 33: 2469–2482
57. Smith MR, Martell EA (1982) Critical stability constants. Plenum, New York
58. Lämmerhofer M, Lindner W (1996) Quinine and quinidine derivatives as chiral selectors I. Brush type chiral stationary phases for high-performance liquid chromatography based on cinchonan carbamates and their application as chiral anion exchangers. J Chromatogr A 741: 33–48
59. Roses M, Bosch E (2002) Influence of mobile phase acid–base equilibria on the chromatographic behaviour of protolytic compounds. J Chromatogr A 982:1–30
60. Adlof R, List G (2004) Analysis of triglyceride isomers by silver-ion high-performance liquid chromatography: effect of column temperature on retention times. J Chromatogr A 1046: 109–113
61. Wu N, Yehl PM, Gauthier D, Dovletoglu A (2004) Retention and thermodynamic studies of piperazine diastereomers in reversed-phase liquid chromatography. Chromatographia 59: 189–195
62. Yogo K, Takemura C, Saito Y, Jinno K (2011) An abnormal temperature dependence of alkylpyrazines' retention in reversed-phase liquid chromatography. Anal Sci 27:1257–1260
63. Matarashvili I, Chankvetadze L, Fanali S, Farkas T, Chankvetadze B (2013) HPLC separation of enantiomers of chiral arylpropionic acid derivatives using polysaccharide-based chiral columns and normal-phase eluents with emphasis on elution order. J Sep Sci 36:140–147